

Exchange biasing in sputtered NiFe/PtMn bilayers

Haiwen Xi,^{a)} Bo Bian, David E. Laughlin, and Robert M. White

Data Storage Systems Center, Carnegie Mellon University, Pittsburgh, Pennsylvania 15213

The exchange coupling between ferromagnetic Ni₈₁Fe₁₉ and antiferromagnetic (AF) Pt_xMn_{1-x} films prepared by rf and dc magnetron sputtering has been investigated. The Pt content in the Pt_xMn_{1-x} film is in the range of 0 at. % x <math>< 20</math> at. %. The exchange field and coercivity were found to depend strongly on the deposition conditions and the AF film composition. X-ray diffraction measurements and transmission electron microscopy measurement showed a γ -PtMn phase with a disordered fcc structure when the Pt_xMn_{1-x} was deposited on top of the Ni₈₁Fe₁₉ layer. The exchange bias was found to depend on the texture and film composition of the γ -PtMn layers.

© 2000 American Institute of Physics. [S0021-8979(00)35608-0]

Intensive studies have been made on exchange biasing materials for their application in anisotropic magnetoresistive (AMR) and giant magnetoresistive (GMR) spin-valve sensors used in high-density recording. Antiferromagnetic (AF) FeMn is commonly used for domain stabilization in AMR sensors and has been well studied.¹ In addition to FeMn, other exchange materials, such as CoNiO, NiMn, IrMn, CrMnPt, and RuRhMn, have been investigated.²⁻⁸ However, little work has been done on the AF PtMn alloy with less than 20 at. % Pt content.⁹ PtMn is of particular interest because of its corrosion resistance. We have investigated the exchange bias between ferromagnetic (FM) Ni₈₁Fe₁₉ and AF Pt_xMn_{1-x} (0 at. % x <math>< 20</math> at. %). In this article, the magnetic properties, which depend on the deposition condition, film texture, and microstructure, will be presented.

Ni₈₁Fe₁₉ and Pt_xMn_{1-x} (PtMn) bilayers were deposited by magnetron sputtering onto glass substrates with a Ta buffer layer in a homemade five target sputtering system. Another 50 Å Ta layer was deposited on the top of the bilayer to protect samples against oxidation in air. The base pressure of the system was typically 10⁻⁷ Torr. The Ni₈₁Fe₁₉ film was sputtered from a permalloy target at an Ar pressure of 4 mTorr and a supply power of 400 W. The PtMn were sputtered from a Mn target with Pt chips bonded to it. The unidirectional exchange anisotropy and the uniaxial anisotropy of the exchange coupled Ni₈₁Fe₁₉ layer were induced by the magnetic field of about 10 Oe arising from the ferrofluid seal on the substrate table in the sputtering chamber during deposition. Exchange biasing was obtained in samples in which the PtMn film was deposited on top of the Ni₈₁Fe₁₉ layer. No exchange bias was observed when the PtMn was deposited first to form the bilayer structure: Sub/Ta/PtMn/Ni₈₁Fe₁₉/Ta.

A $B-H$ loop tracer with a frequency of 10 Hz was used to characterize the magnetic properties of the films at room temperature. The Pt content of the Pt_xMn_{1-x} films was measured by energy dispersion x-ray fluorescence measurements. The crystallographic properties of the thin film samples were determined using x-ray diffraction (XRD). $\theta-2\theta$ scanning

was performed on a Rigaku diffractometer using a Cu $K\alpha$ radiation source. Transmission electron microscopy (TEM) was used to examine the microstructure of the PtMn films.

Usually the exchange bias is measured by a hysteresis loop method. An exchange field H_e , i.e., shift of the hysteresis loop of the biased FM film relative to a single FM film, and a coercivity H_c , i.e., the half width of the loop, are used to characterize the exchange bias effect. Figure 1 illustrates the general dependencies of the exchange field and coercivity of the Ni₈₁Fe₁₉(250 Å)/PtMn(300 Å) bilayers with PtMn films prepared by rf magnetron sputtering at different deposition conditions. An exchange field as high as 37.7 Oe for 250 Å Ni₈₁Fe₁₉ was achieved under the conditions of 100 W power and 20 mTorr pressure. Decreasing the pressure and increasing the power results in a decrease of the exchange

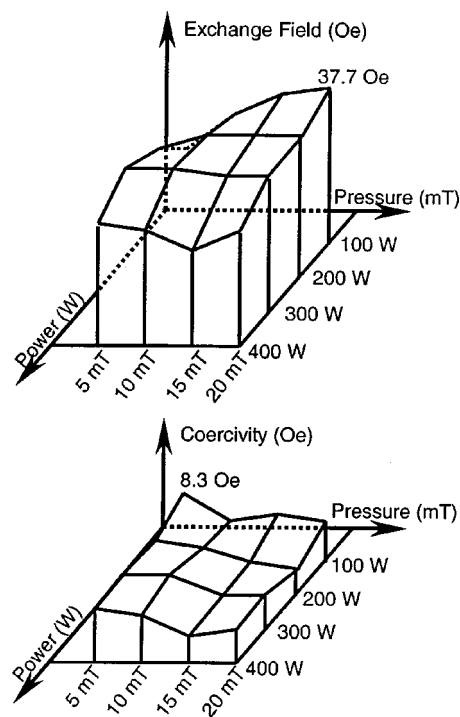


FIG. 1. Effect of the sputtering condition on the exchange field H_e and coercivity H_c . The PtMn layers were deposited using rf magnetron sputtering. The Ni₈₁Fe₁₉ layer thickness is 250 Å.

^{a)}Electronic mail: hxi@andrew.cmu.edu

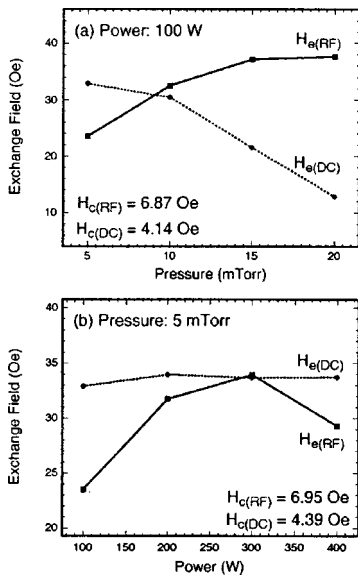


FIG. 2. Contrast between the exchange bias of PtMn layers prepared by rf and dc magnetron sputtering.

field. It was found that the coercivity changes more with the power than with the pressure. Increasing the power decreases the coercivity. In the range we investigated, the highest coercivity 8.3 Oe, was found in the bilayer with the PtMn film sputtered at 100 W power and 5 mTorr pressure, while the exchange field had a low value of 23 Oe for a Pt content of 6 at. %.

Comparison of the exchange bias from rf magnetron sputtered and dc magnetron sputtered samples is shown in Fig. 2. dc magnetron sputtering gives a larger deposition rate than rf magnetron sputtering does. Unlike the bilayer system prepared by rf magnetron sputtering, the system prepared by dc magnetron sputtering shows a decrease of the exchange field with increasing pressure when the power is 100 W. Keeping the pressure at 5 mTorr for dc magnetron sputtering, the exchange field changes little with the power. A study of the exchange bias in $Ni_{81}Fe_{19}/Ir_{20}Mn_{80}$ bilayers, which were prepared in the same sputtering system, showed that an almost 50% higher exchange field can be achieved by using dc magnetron sputtering than by using rf magnetron sputtering.¹⁰ We did not see such an exchange field improvement in our $Ni_{81}Fe_{19}/PtMn$ system. However, the samples prepared by dc magnetron sputtering show much smaller and less condition-dependent coercivity than those produced by rf magnetron sputtering. The average values of coercivity obtained from both rf and dc magnetron sputtering are shown in Fig. 2, suggesting that higher deposition rates give smaller coercivity.

The PtMn film composition changes with the sputtering conditions. Figure 3 shows the pressure and power dependence of the film composition and the exchange field. The Pt content in PtMn films increases with increasing pressure and increasing power during rf magnetron sputtering. The exchange field increases as the Pt content increases up to 10 at. % and then decreases with further increasing of the Pt content. This Pt content dependence of the exchange field is consistent with the results obtained by keeping the sputtering

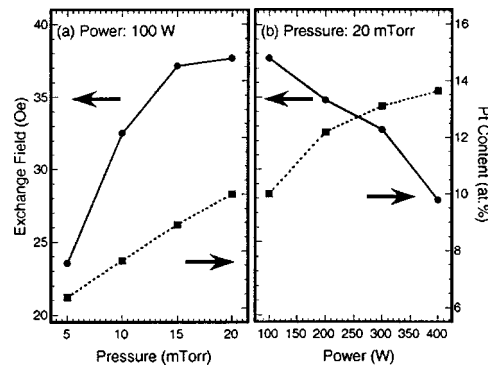


FIG. 3. Relationship between the exchange bias and the PtMn film composition.

power at 100 W and the pressure at 20 mTorr but changing the Pt chip number in the target.

Figure 4 shows the XRD data for the $Ni_{81}Fe_{19}/PtMn$ bilayers with PtMn layers deposited at a pressure of 5, 10, 15, and 20 mTorr with the power fixed at 100 W. A strong (111) texture for the fcc $Ni_{81}Fe_{19}$ was found. The peak shown in Fig. 4 around 41° is due to PtMn. The γ phase for pure Mn with the fcc structure is only stable between 1079 and 1140 K, but γ -Mn can be produced by doping with other elements at room temperature.¹¹ From electron diffractions of $Ni_{81}Fe_{19}/PtMn$ bilayer samples, a γ -PtMn with a disordered fcc structure was always found in samples with the Pt content in the range of 6 at. % $<x < 19$ at. %. An α -Mn phase was also found in samples with a small amount of Pt doping (e.g., 6 at. % Pt). In principle, PtMn films can form in a γ' -PtMn phase with a type of Cu_3Au structure as the Pt to Mn composition ratio gets close to 1:3.¹² However, there is little evidence for the existence of γ' -PtMn phase in the samples that we investigated. XRD measurements show that the (111) planes of the γ -PtMn phase grow on the $Ni_{81}Fe_{19}$. For comparison with our $Ni_{81}Fe_{19}/PtMn$ bilayers, TEM mea-

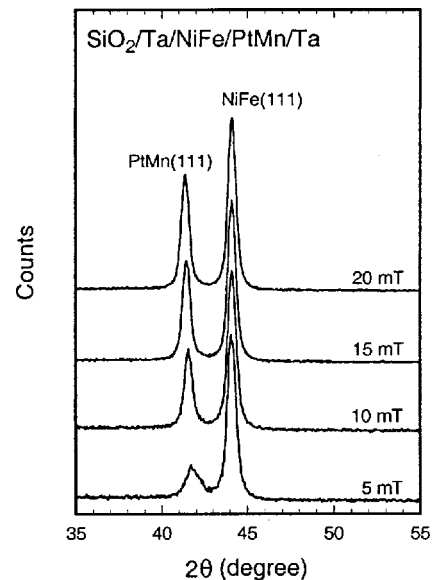


FIG. 4. XRD patterns of the $Ni_{81}Fe_{19}(250 \text{ \AA})/PtMn(300 \text{ \AA})$ bilayer films with Pt_xMn_{1-x} layers deposited at different pressures while the power is fixed at 100 W.

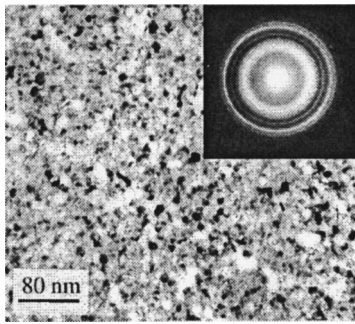


FIG. 5. Bright-field TEM image and electron diffraction pattern of the $\text{Pt}_{10}\text{Mn}_{90}$ layer in the $\text{Ni}_{81}\text{Fe}_{19}(150 \text{ \AA})/\text{Pt}_{10}\text{Mn}_{90}(450 \text{ \AA})$ sample.

measurements on exchange biased $\text{Ni}_{81}\text{Fe}_{19}/\text{Ir}_{20}\text{Mn}_{80}$ samples were also carried out. Only the disordered γ -IrMn phase was found. The ordered γ' -IrMn phase was absent.

There is a strong correlation between the film texture and film composition. The (111) texture is shown by XRD to increase with Pt content in the range from 0 to 20 at. %. The exchange bias is an interfacial exchange coupling. However, the intrinsic magnetic properties, the crystal structure and orientation, and the microstructure of the AF layer can affect the exchange bias.^{13,14} Previous experiments have shown that texture enhancement leads to an improvement of the exchange bias.^{15,16} In particular, an increase of the exchange field and a decrease of the coercivity in $\text{Ni}_{81}\text{Fe}_{19}/\text{Fe}_{50}\text{Mn}_{50}$ bilayers can be achieved by improving the γ - $\text{Fe}_{50}\text{Mn}_{50}$ (111) texture.¹⁶ In our $\text{Ni}_{81}\text{Fe}_{19}/\text{PtMn}$ system, the (111) texture of the γ -PtMn is not well established when the Pt content is too low, resulting in a smaller exchange field and a larger coercivity. When the (111) texture of the γ -PtMn increases with increasing Pt content, the exchange bias is improved. However, when the Pt content is higher than 10 at. %, the exchange field decreases with improving of the γ -PtMn (111) texture. We suggest that this is associated with the fact that the exchange bias is strongly dependent on the intrinsic properties of the antiferromagnet such as the exchange coupling between the AF moments and its uniaxial anisotropy.^{13,14} Thus, although the γ -PtMn (111) texture is improved with increasing of Pt content, the exchange coupling constant A_{AF} or the anisotropy K_{AF} of the PtMn decreases with Pt content as evidenced by the fact that the magnetic moment and Néel temperature of Mn alloys with the γ -phase are experimentally found to decrease with dopant concentration.¹¹

Specimens for TEM observation were taken from an as-deposited $\text{Si}/\text{Ta}(50 \text{ \AA})/\text{Ni}_{81}\text{Fe}_{19}(150 \text{ \AA})/\text{Pt}_{10}\text{Mn}_{90}(450 \text{ \AA})/\text{Ta}(50 \text{ \AA})$ sample. Figure 5 shows an electron diffraction pattern as well as a TEM plane view bright-field image of the $\text{Pt}_{10}\text{Mn}_{90}$ layer. The $\text{Pt}_{10}\text{Mn}_{90}$ grains in this image appear to be equiaxial. The TEM image shows an average grain size of about 100 \AA .

TABLE I. Summary of the properties of $\text{Pt}_{10}\text{Mn}_{90}$ as an exchange bias material coupled with $\text{Ni}_{81}\text{Fe}_{19}$. The exchange field H_e is for 250 \AA $\text{Ni}_{81}\text{Fe}_{19}$. The minimum thickness t_{min} is the thickness necessary for the $\text{Pt}_{10}\text{Mn}_{90}$ to pin the $\text{Ni}_{81}\text{Fe}_{19}$ layer. The blocking temperature T_B is the temperature at which the exchange bias vanishes.

H_e (Oe)	t_{min} (\AA)	ρ_{PtMn} ($\mu\Omega \text{ cm}$)	T_B ($^{\circ}\text{C}$)
38	100	410	160

Some parameters of the $\text{Pt}_{10}\text{Mn}_{90}$ as an exchange bias material are summarized in Table I. PtMn shows properties similar to $\text{Fe}_{50}\text{Mn}_{50}$ and $\text{Ir}_{20}\text{Mn}_{80}$.¹⁷ Compared with γ - $\text{Fe}_{50}\text{Mn}_{50}$, PtMn has almost the same exchange field and blocking temperature, slightly larger minimum thickness, and remarkably larger resistivity.¹⁰ It is interesting to note that the minimum thickness to pin the $\text{Ni}_{81}\text{Fe}_{19}$ layer for $\text{Pt}_{10}\text{Mn}_{90}$ is the same as the $\text{Pt}_{10}\text{Mn}_{90}$ grain size. This relationship sheds light on exchange biasing in a polycrystalline bilayer where the exchange coupling is between the FM magnetization and the AF grains at the interface¹⁴ and is discussed elsewhere.¹⁸

This work is supported by the National Science Foundation under Grant No. ECD-8907068.

- ¹R. D. Hempstead, S. Krongelb, and D. A. Thompson, IEEE Trans. Magn. **14**, 521 (1978).
- ²M. Carey and A. E. Berkowitz, Appl. Phys. Lett. **60**, 3060 (1992).
- ³T. Lin, D. Mauri, N. Staud, C. Hwang, J. K. Howard, and G. L. Gorman, Appl. Phys. Lett. **65**, 1183 (1994).
- ⁴M. Konoto, M. Tsunoda, and M. Takahashi, J. Appl. Phys. **85**, 4925 (1999).
- ⁵Nakatani, H. Horoyuki, K. Hoshino, and Y. Sugita, J. Magn. Magn. Mater. **173**, 321 (1997).
- ⁶S. Soeya, H. Hoshiya, M. Fuyama, and S. Tadokoro, J. Appl. Phys. **80**, 1006 (1996).
- ⁷H. Xi and R. M. White, J. Appl. Phys. **87**, 410 (2000).
- ⁸S. Araki, E. Omata, M. Sano, M. Ohta, K. Noguchi, H. Morita, and M. Matsuzaki, IEEE Trans. Magn. **34**, 387 (1998).
- ⁹M. Saito, Y. Kakaiharu, T. Watanabe, and N. Hasegawa, J. Magn. Soc. Jpn. **21**, 505 (1997).
- ¹⁰A. J. Devasahayam, Ph.D. thesis, Carnegie Mellon University, June 1998.
- ¹¹D. Meneghetti and S. S. Sidhu, Phys. Rev. **105**, 130 (1957); Y. Endoh and Y. Ishikawa, J. Phys. Soc. Jpn. **30**, 1614 (1971).
- ¹²E. Krén, G. Kádár, L. Pál, J. Sólyom, P. Szabó, and T. Tarnóczy, Phys. Rev. **171**, 574 (1968).
- ¹³C. Mauri, H. C. Siegmann, P. S. Bagus, and E. Kay, J. Appl. Phys. **62**, 3047 (1987); A. P. Malozemoff, Phys. Rev. B **35**, 3679 (1987); J. Appl. Phys. **63**, 3874 (1988); Phys. Rev. B **37**, 7673 (1988).
- ¹⁴M. D. Stiles and R. D. McMichael, Phys. Rev. B **59**, 3722 (1999).
- ¹⁵A. J. Devasahayam and M. H. Kryder, IEEE Trans. Magn. **31**, 3820 (1995).
- ¹⁶G. Choe and S. Gupta, Appl. Phys. Lett. **70**, 1766 (1997); IEEE Trans. Magn. **33**, 3691 (1997).
- ¹⁷M. Lederman, IEEE Trans. Magn. **35**, 794 (1999).
- ¹⁸H. Xi, K. R. Mountfield, and R. M. White, J. Appl. Phys. (submitted)